THE EFFECTS OF B2 STRUCTURED UNDERLAYERS ON THIN FILM MAGNETIC RECORDING MEDIA

LI-LIEN LEE*, D. E. LAUGHLIN** AND D. N. LAMBETH**

*INTEVAC, INC. 3550 Bassett Street, Santa Clara, CA 95054, **Data Storage Systems Center, Carnegie Mellon University, Pittsburgh, PA 15213

ABSTRACT

It is well known that underlayers have profound effects on the magnetic properties of longitudinal thin film media. These effects are derived from the underlayer's influence on the structural features of the magnetic media such as crystallographic texture, grain size and grain isolation. Pure Cr has been the most popular underlayer for Co alloy thin films for more than two decades mainly because Cr underlayers can enhance the c-axis in-plane crystallographic texture of the overlying Co alloy thin films. Many investigators have studied alternative underlayers and have achieved various degrees of success. However, those underlayers are seldom different from the BCC structure or are Cr with various alloying additions. We have studied NiAl and FeAl underlayers with the B2 ordered structure (CsCl prototype) which have lattice constants similar to that of Cr. RF diode sputter deposited NiAl and FeAl films were found to have the B2 structure and have a smaller grain size and more uniform equiaxed grains compared to that of a similarly deposited Cr film. X-ray diffractometry studies showed that CoCrPt films grown on NiAl or FeAl underlayers tend to have the $(10\bar{1}0)$ crystallographic texture with a better in-plane c-axis orientation than CoCrPt films grown on Cr underlayers. The in-plane coercivities of the CoCrPt/NiAl and CoCrPt/FeAl films can be significantly improved by inserting a thin intermediate layer of Cr between the CoCrPt and its underlayer. Cr, NiAl and FeAl underlayers are found to have a strong (002) crystallographic texture when sputter deposited MgO seed layers are used. The MgO seed layers increase the coercivities of the CoCrPt films having Cr or NiAl underlayers but decrease the coercivities of the CoCrPt films having FeAl underlayers.

INTRODUCTION

Longitudinal magnetic recording media for hard drives are usually multilayered thin films. The properties of such thin films depend mainly on the choice of the hard magnetic layer and the underlayer. Pure Cr has been the most often used underlayer for Co alloy thin films for more than two decades. One of the important reasons for the popularity of Cr is its ability to induce grain-to-grain epitaxial growth of the overlying Co alloy such that the c-axis, the magnetization easy direction,

of the Co layer can lie predominately in the plane of the film. The heteroepitaxial relationships between Cr and Co which bring the Co c-axis into or close to the film plane were found to be $(112)_{Cr}$ // $(1\bar{0}10)_{Co}$, $(002)_{Cr}$ // $(1\bar{1}20)_{Co}$ and $(110)_{Cr}$ // $(1\bar{0}\bar{1}1)_{Co}$ [1]. Many investigations have been performed on the Cr underlayer since it was first used as an underlayer for Co alloy longitudinal thin film media almost three decades ago [2-9].

The Cr underlayer has been so successful in satisfying the high coercivity and low noise needs of the Co based alloy thin film media, that alternative underlayers have been constantly overlooked. Although many materials have been studied as alternative underlayers for Co based alloy longitudinal thin films, most of them have the BCC crystal structure or are merely Cr based alloys with minor alloy additions. Recently, there has been a trend of adding higher concentrations of the alloying element, such as V, Ti and Mo to better accommodate the expanded lattice of the CoCrPt alloy which has a large Pt content. However, these Cr alloy underlayers are still not very different from the pure Cr underlayers.

Although it is believed that differences in crystal structure, bonding and materials properties all play important roles in heteroepitaxy, there is still not enough fundamental understanding of the epitaxy between dissimilar materials. In most studies, the major concern has been with the differences in lattice parameters between the two materials. The technique for achieving the epitaxial orientation is experimentally determined by trial and error.

To emulate the success of the Cr underlayer, we have selected materials having a crystal structure similar to the BCC Cr in hope of creating better underlayers. The B2 ordered crystal structure (space group $P m \bar{3} m$) is a derivative of the BCC (A2) structure. If we disregard the differences among the atoms, the B2 and BCC have the same structure. A material which has the B2 structure and a lattice constant close to that of the Cr, ~0.288 nm, is likely to induce a similar epitaxial growth of the Co alloy as that grown on a Cr underlayer. Nevertheless, prior to our work [10] B2 structure materials were never studied as underlayers in thin film recording media.

A search of Pearson's Handbook [11] suggested that NiAl and FeAl may be potential candidates for alternative underlayers. Both the NiAl and FeAl B2-ordered intermetallic phases and appear to be stable over wide composition ranges in their respective binary phase diagrams. Stoichiometric NiAl and FeAl are nonmagnetic and have lattice constants of 0.288 nm and 0.291 nm respectively. The strong bonding between closest neighboring atoms in these B2 intermetallic phases may create interesting microstructures (e.g. smaller grain size) and crystallographic textures in the sputter deposited thin films. It is of interest to know if these materials can be deposited to form the right kind of thin film texture to induce the c-axis of the Co layer to lieclose to the film plane. Whether these B2 intermetallic phases can be suitable underlayers for Co alloy longitudinal thin film media is a question which was begging for an answer.

In this paper, we will review our work to date and our understandings of the NiAl and FeAl underlayers which also include studies on intermediate layers and seed layers [12-15].

EXPERIMENT

All films in this study were prepared by a 3-target RF diode sputtering system. Multilayered films can be deposited without breaking the vacuum. Targets used included CoCrPt, Cr, NiAl, FeAl and MgO. Substrates were 1-inch square smooth Corning 7059 glass coupons. Sputtering was performed at a fixed AC power of 100 watts (2.3 W/cm^2). All the CoCrPt films presented in this paper were sputtered onto substrates which were RF biased by a -100 V. All the nonmagnetic films were deposited without substrate bias. Base pressures were at least 5 x 10^{-7} Torr before film deposition. Argon sputtering pressures were kept at 10 mTorr. Inductively coupled plasma (ICP) analysis revealed the CoCrPt films had a composition of 78.5 at% Co, 9 at% Cr and 12.5 at% Pt. The NiAl films had 52 at% Al and 48 at% Ni and the FeAl films were 52 at% Fe and 48 at% Al.

Film microstructures were studied by transmission electron microscopy (TEM), atomic force microscopy (AFM) and by symmetrical x-ray diffractometry θ-2θ scan with the Cu Kα radiation. The in-plane bulk magnetic properties of the thin films were measured by vibrating sample magnetometry (VSM). A magnetic field of up to 10 kOe was applied in the film plane, which was large enough to saturate the magnetization. All films were prepared without an overlayer or overcoat.

RESULTS

B2 underlayers

The NiAl and FeAl films were found to have the B2 structure by TEM electron diffraction when the films were sputter-deposited directly onto glass substrates. The lattice constants of the NiAl and FeAl films were found to be 0.289 nm and 0.290 nm respectively, measured by x-ray diffractometry. AFM studies (not shown) revealed that the NiAl and FeAl films have a surface smoothness better or comparable to that of a similarly deposited Cr film. Fig. 1 shows the plan view TEM bright field micrographs of 100 nm thick NiAl and FeAl films which are deposited on smooth glass substrates without intentional substrate heating. Both the NiAl and FeAl films have uniform equiaxed grains of about 15 nm in diameter which is about half the grain size of a similarly deposited Cr film. Because the medium limited signal-to-noise power ratio (SNR) is proportional to the number of magnetically isolated grains within a bit cell, these B2 films with smaller grains show great promise as underlayers.

Of comparable importance to the grain size is the crystallographic texture of the NiAl and FeAl films. This was the second thing which came to our attention. It is easier to compare thin film textures of different materials by comparing their texture evolution as the films grow. The x-ray diffraction spectra of NiAl, FeAl and Cr of various thicknesses deposited on smooth glass substrates are plotted in Figs. 2, 3 and 4. These figures show that both the NiAl and FeAl films have a stronger (112) texture than the Cr film. The (112) lamellar texture becomes more observable as the B2 films grow

thicker. However, the (112) peaks in the x-ray diffraction spectra of similarly prepared Cr films are either too weak to be observed or the texture does not exist. This difference in film texture results in differing induced Co-alloy texture and resulting magnetic properties.

Fig. 5 compares the coercivity vs. underlayer thickness plots of 40 nm thick CoCrPt films deposited on NiAl and Cr underlayers. Fig. 6 is a similar plot for the films with the FeAl underlayers. The CoCrPt films on NiAl and FeAl underlayers show gradual and continuous increase of Hc as the underlayers thicken, while the CoCrPt/Cr films have a steep Hc increase in the thin Cr region and then the Hc levels off. This is probably related to the difference in grain size and crystallographic texture of the CoCrPt films as different underlayers are used.

Fig. 7, 8 and 9 show the x-ray diffraction spectra of 40 nm thick CoCrPt films on various thicknesses of NiAl, FeAl and Cr underlayers respectively. It is found that $(10\bar{1}0)$ Co peaks are present in all the CoCrPt/NiAl and CoCrPt/FeAl films whereas $(10\bar{1}0)$ Co peaks are much weaker in the CoCrPt/Cr films. The $(10\bar{1}0)$ Co is believed to grow epitaxially on the (112) NiAl and FeAl. The visible (0002) Co peaks in Fig. 9 (but not in Fig. 7 and 8) indicate an inferior in-plane c-axis texture of the CoCrPt/Cr film. This is perhaps because the Pt rich CoCrPt alloy has an expanded lattices. This makes it difficult to obtain the $(10\bar{1}1)$ // (110) epitaxial growth. However, the lattice expansion is apparently not large enough to affect the $(10\bar{1}0)$ // (112) epitaxy.

Intermediate layers

The CoCrPt/NiAl films have better in-plane c-axis texture than the CoCrPt/Cr films, however, this occurs without the benefit of higher in-plane coercivities. Of course while the fact that CoCrPt/NiAl has smaller grain size may be part of the reason for this, we believe that the interface structure of the CoCrPt/NiAl also may be less favorable for high Hc. This can be changed by inserting an intermediate layer between the CoCrPt and the NiAl. Because Cr and NiAl have similar crystal structures and lattice constants as previously stated, use of Cr as an intermediate layer for the CoCrPt/NiAl may not change epitaxial relationship between the NiAl underlayer and the CoCrPt layer.

NiAl (100 nm), Cr (2.5 nm) and CoCrPt (40 nm) layers were sequentially deposited onto a smooth glass substrate without breaking the vacuum of the sputtering system. A comparison of bulk magnetic properties of the films with and without the intermediate layers are listed in Table I. It is found that the Cr intermediate layer increases the Hc of the CoCrPt/NiAl by ~75 %. S and S* values also show significant increase.

Fig. 10 shows the in-plane coercivities of various thicknesses of CoCrPt films on 100 nm thick Cr underlayers and on 100 nm thick NiAl underlayers with and without a 2.5 nm Cr intermediate layer. The film with a Cr intermediate layer and NiAl underlayer always has the highest Hc. TEM studies of cross sectional specimens showed no grain coarsening caused by the Cr intermediate layer. A similar effect of the Cr intermediate layer can be found in the CoCrPt/FeAl films. Fig. 11 shows the

in-plane coercivities of 40 nm thick CoCrPt films on various thicknesses of FeAl underlayers with and without a 2.5 nm Cr intermediate layer. A greater than 20 % increase in coercivity is observed in all CoCrPt/FeAl films by inserting the Cr intermediate layer. X-ray diffractometry studies show the $(1\bar{0}10)$ textures of the CoCrPt films are enhanced by the addition of the Cr intermediate layer. This stronger $(1\bar{0}10)$ texture may arise from the increase in adatom mobility of the Co, Cr or Pt atoms as they come into contact with the Cr instead of the NiAl or FeAl during the sputtering process. Higher atomic mobility favors better grain-to-grain epitaxial growth. On the other hand, introducing Cr atoms to the interface may also help increase the intergranular segregation of Cr in the CoCrPt layer by means of interdiffusion [16], which would enhance its coercivity.

Seed layers

We have deposited NiAl and FeAl films onto preheated substrates trying to change their textures. However, unlike the Cr, the (002) texture growth can not be obtained. The coercivities of the CoCrPt/NiAl and CoCrPt/FeAl films do not increase when the substrates are heated prior to the deposition. This appears to be due to the heat diminisheing the (112) texture in the B2 underlayer. Two kinds of seed layers, MgO and Cr, were used to induce (002) texture in the NiAl and FeAl. A previous study showed that sputtered MgO seed layers can induce (002) growth in Cr films [17]. It was believed that a MgO seed layer should also induce (002) texture in NiAl and FeAl films. Likewise, (002) textured Cr films obtained by depositing on a preheated substrate was also used for this purpose.

The in-plane bulk magnetic properties of the CoCrPt(40 nm)/NiAl(100 nm) films on various thicknesses of MgO are listed in Table II. MgO seed layers are shown to induce higher coercivity. The x-ray diffractometry studies show that MgO seed layers indeed can induce the (002) lamellar texture in the NiAl films (Fig. 12). The (002) peak intensity in the spectra increases initially and then decreases as the MgO becomes thick (>10 nm). The deterioration of the (002) texture as the MgO grows thicker is found to be caused by the film's roughening effect. It was found, from AFM studies, that the MgO surface roughness increases rapidly when the MgO films are thicker than 10 nm. It is apparent that the (002) NiAl // (002) MgO epitaxy is correlated with the MgO film's roughness. A rougher MgO surface has less suitable area for the (002) NiAl to grow on despite the fact that the MgO is still (002) textured. This surface roughening is undesired for the (002) underlayer texture, however, it might be used to induce mechanical sputtered texture on smooth glass disks to avoid stiction of the head slider to the disk [18].

It can be observed that the x-ray spectra in Fig. 12 do not have any CoCrPt diffraction peaks. These CoCrPt films may still have preferred orientation since the x-ray θ-2θ scan can only detect low indices atomic planes parallel to the film surface. If the crystallographic texture of the film is such that there are no atomic planes parallel to the film or if a smaller wavelength x-ray is needed to detect the atomic planes, the θ-2θ scan will not produce any diffraction peaks. Hence TEM studies of the CoCrPt/NiAl films on (002) MgO single crystals 9) were performed and it was found that the CoCrPt

film grew epitaxially on the (002) NiAl. The epitaxial relationship is $[10\bar{1}1]$ CoCrPt // [001] NiAl and $(\bar{1}2\bar{1}0)$ CoCrPt // (200) NiAl. This indicates that the CoCrPt film grown on a (002) texture polycrystalline NiAl film has the $[10\bar{1}1]$ fibrous texture. A $[10\bar{1}1]$ fibrous textured CoCrPt film does not have low indices atomic planes parallel to the film surface and its c-axis lies 47° out of the film plane.

Similar to the NiAl case, the MgO seed layer also induces a strong (002) texture in the FeAl film. However, the coercivity of the CoCrPt/FeAl film decreases ~20 % because of the use of MgO seed layer. This is because the (002) FeAl can only induce a weak $(\bar{1}1\bar{2}0)$ textured CoCrPt which is not as strong as the $(\bar{1}0\bar{1}0)$ texture in the CoCrPt film deposited on (112) textured FeAl. Fig. 13 plots the diffraction spectra of CoCrPt/FeAl and CoCrPt/NiAl films on 8 nm MgO seed layers along with portions of the slower scans to show different intensities of the $(\bar{1}1\bar{2}0)$ Co peak. It is clear that the CoCrPt/FeAl film has a weak $(\bar{1}1\bar{2}0)$ peak while the CoCrPt/NiAl has none. The higher Hc of the CoCrPt/NiAl film than the CoCrPt/FeAl film in Fig. 13 is probably due to the better c-axis inclination of the former film. However, this will not be easily clarified until a better way to quantify the texture is developed.

Table III lists the in-plane magnetic properties of two CoCrPt(40 nm)/NiAl(100 nm) films deposited on 260°C preheated glass substrates with and without a 10 nm Cr seed layer. Higher Hc is observed when the Cr seed layer film is used. Similarly, when the MgO seed layer film is used the x-ray diffraction spectrum of the CoCrPt/NiAl film on the (002) textured Cr seed layer shows no $(\bar{1}1\bar{2}0)$ peak. There are also no surprises in the studies of the (002) Cr seeded CoCrPt/FeAl films. These films have a weak $(\bar{1}1\bar{2}0)$ Co texture and low coercivities. The Cr seed layer studies further confirm that (002) textured NiAl and FeAl underlayers do not yield the same epitaxially growth of the CoCrPt.

Since small grain size is important in obtaining low noise recording media, it is of interest to know whether the Cr and MgO seed layers cause any B2 underlayer grain coarsening. Fig 14 shows TEM micrographs of 100 nm thick NiAl films on different seed layers. The 5 nm thick Cr seed layer causes the NiAl grains to coarsen considerable while the MgO seed layer only has a minimal grain coarsening effect. One might think that this is because the NiAl film deposited on the Cr seed layer has been heated while the NiAl film deposited on the MgO seed layer has not. However, the TEM micrograph of a 100 nm NiAl deposited on a 260°C preheated substrate also shows no signs of grain coarsening (Fig. 15). Therefore, we believe that the commonly used (002) textured Cr film obtained from substrate preheating has a coarse grain structure which should be avoided.

One of our studies was to investigate the difference in crystallographic texture of the CoCrPt film when the Cr, NiAl and FeAl underlayers used are thinner than 5 nm. Referring to Fig. 5 and 6, one can see that the in-plane Hc of the CoCrPt/Cr film drops abruptly in this region. What is happening to the crystallographic texture of the film is included here as a final note.

6

Fig. 16 shows the x-ray diffraction spectra of 40 nm thick CoCrPt films on Cr underlayers ranging from 0 to 50 Å on smooth glass substrates. It is found that the (0002) CoCrPt intensity initially increases as the Cr thickness decreases. The CoCrPt film has the strongest (0002) texture when the Cr underlayer is ~25Å thick. As the Cr underlayer thickness decreases further, the degree of the (0002) texture also decreases. This shows that the CoCrPt film sputtered on bare glass does not have a strong (0002) texture and there is a critical Cr underlayer thickness to produce the strongest perpendicular oriented CoCrPt film.

The existence of a non-zero critical underlayer thickness for the best perpendicularly orientated Co alloy also occurs in the film with the FeAl and NiAl underlayers (Fig. 17, 18). However, the critical thickness is lower (~10 Å) and the highest achievable (0002) peak intensity is different. This finding points to a new possibility of achieving a perpendicular medium by using a very thin underlayer.

CONCLUSIONS

(1) Sputter deposited NiAl and FeAl were found to have the B2 crystal structure and the (112) crystallographic texture. The grain size of the NiAl and FeAl films is smaller than that of a similarly deposited Cr film. The small grain size is beneficial to the SNR of the media. The CoCrPt films deposited on NiAl and FeAl underlayers were found to have the $(1\bar{0}\bar{1}0)$ lamellar texture through epitaxial growth with the (112) textured underlayer.

(2) Intermediate layers of Cr can improve the coercivities of the CoCrPt/NiAl and CoCrPt/FeAl films. This improvement is attributed to the better in-plane c-axis texture of the CoCrPt film and possible Cr interdiffusion from the intermediate layer.

(3) Sputter deposit NiAl or FeAl films onto preheated substrates do not produce the (002) texture. A sputter deposited MgO seed layer can be used to induce (002) texture growth in the NiAl and FeAl film without the need of substrate preheating. A (002) textured underlayer can induce higher coercivity in the CoCrPt/NiAl film, but not in the CoCrPt/FeAl film.

(4) The (002) textured Cr films deposited on preheated substrates can also be used as seed layers for the NiAl and FeAl, however, they also induce grain coarsening.

(5) Through proper selection and processing of the intermediate layer, underlayer and seed layer, the magnetic properties of the thin film medium can be optimized.

ACKNOWLEDGMENT

REFERENCES

1   K. Hono, B. Wong and D. E. Laughlin: J. Appl. Phys., **68**, 1990, p. 4834.

2   J. Daval and D. Randet: IEEE Trans. Magn., **6**, 1970, p. 768.

3   S. L. Duan, J. O. Artman, J. W. Lee, B. Wong and D. E. Laughlin: IEEE Trans. Magn., **25**, 1989, p. 3847.

4   T. Yogi, G. L. Gorman, C. Hwang, M. A. Kakalec and S. E. Lambert: IEEE Trans. Magn., **24**, 1988, p. 2727.

5   J. L. Presseky, S. Y. Lee, N. Heiman, D. Williams, T. Coughlin and D. E. Speliotis: IEEE Trans. Magn., **26**, 1990, p. 1596.

6   Y. Hsu, J. M. Sivertson and J. Judy: IEEE Trans. Magn., **26**, 1990, p. 1599.

7   M. F. Doerner, P.-W. Wang, S. M. Mirzamaani and D. S. Parker: Mat. Res. Soc. Proc., **232**, 1991, p. 27.

8   K. E. Johnson, M. R. Kim and S. Guruswamy: IEEE Trans. Magn., **28**, 1992, p. 3099.

9   L. Tang and G Thomas: J. Appl. Phys., **74**, 1993, p. 5025.

10   L.-L. Lee, D. E. Laughlin and D. N. Lambeth, IEEE Trans. Magn., **30**, 1994, p. 3950.

11   P. Villars and L. D. Calvert: *Pearson's Handbook of Crystallographic Data for Intermetallic Phases* (American Society for Metals, Metals Park, 1991) 2nd ed., Vol. 1.

12   L.-L. Lee, D. E. Laughlin, L. Fang and D. N. Lambeth: IEEE Trans. Magn., **31**, 1995, p. 2728.

13   L.-L. Lee, D. E. Laughlin and D. N. Lambeth, J. Appl. Phys., **79**, 1996, p. 4902.

14   L. Tang, L.-L. Lee, D. E. Laughlin and D. N. Lambeth: Appl. Phys. Lett., **69**, 1996, p. 1163.

15   L.-L. Lee, D. E. Laughlin and D. N. Lambeth: J. Appl. Phys., **81**, 1997, p. 4366.

16   Y. C. Feng, D. E. Laughlin and D. N. Lambeth: IEEE Trans. Magn., **30**, 1994, p. 3948.

17   L.-L. Lee, B. K. Cheong, D. E. Laughlin and D. N. Lambeth: Appl. Phys. Lett., **67**, 1995, p. 3638.

18   M. Mirzamaani, C. V. Jahnes and M. A. Russak, IEEE Trans. Magn., **28**, 1992, p. 3090.

Table I
The in-plane magnetic properties of CoCrPt(40 nm)/Cr(100 nm) and CoCrPt(40 nm)/NiAl(100 nm) with and without a 2.5 nm Cr intermediate layer

Underlayer	H_c (Oe)	S (M_r/M_s)	S*	$M_r t$ (memu/cm^2)
Cr	2250	0.86	0.85	1.34
NiAl	1850	0.84	0.88	1.36
Cr/NiAl	3290	0.90	0.95	1.34

Table II
In-plane magnetic properties of CoCrPt(40 nm)/NiAl(100 nm) on MgO seed layers of various thicknesses

MgO thickness (nm)	H_c (Oe)	S (M_r/M_s)	S*	$M_r t$ (memu/cm^2)
0	1862	0.87	0.84	1.4
2	2558	0.92	0.86	1.2
5	2811	0.92	0.87	1.2
10	3238	0.91	0.87	1.0
20	3236	0.86	0.84	1.0
50	3182	0.82	0.87	1.0

Table III
In-plane magnetic properties of CoCrPt(40 nm)/NiAl(100 nm) films on 260°C preheated glass substrates with and without a 10 nm Cr seed layer

Underlayer	H_c (Oe)	S (M_r/M_s)	S*	$M_r t$ (memu/cm^2)
NiAl	2220	0.81	0.79	0.81
NiAl/Cr	3150	0.85	0.78	0.85
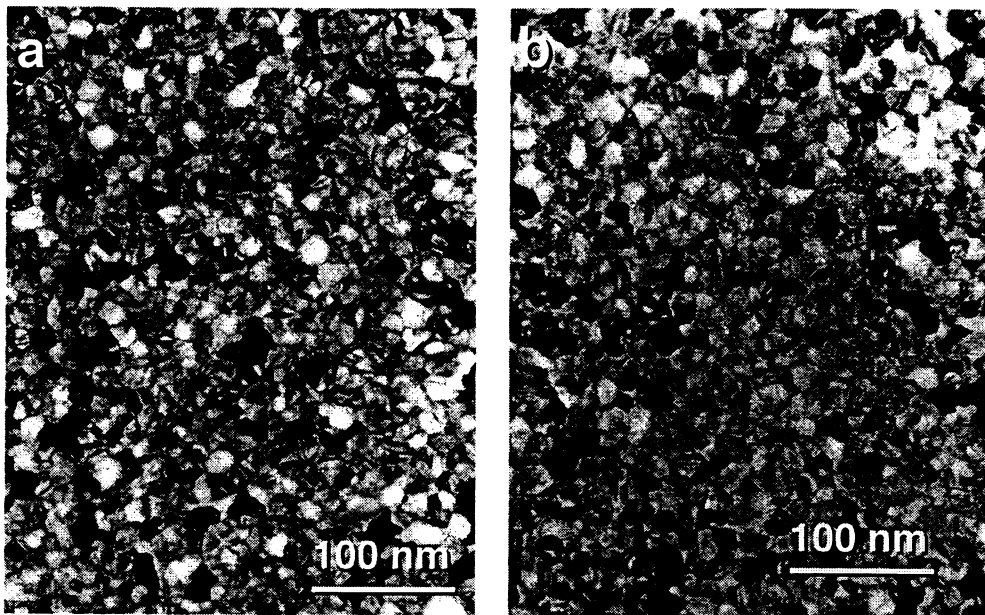
Fig. 1 Plan-view TEM bright field micrographs of 100 nm thick (a) NiAl film and (b) FeAl film.
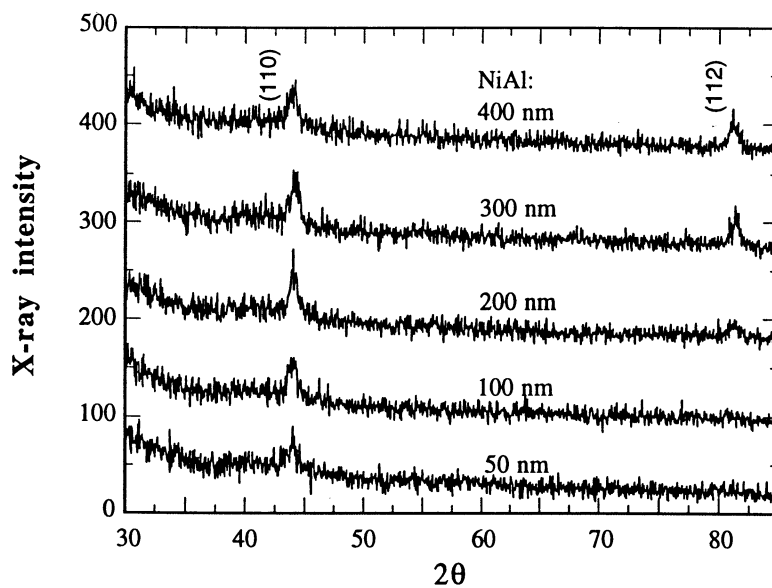
Fig. 2 The evolution of the crystallographic texture of NiAl films on smooth glass substrates.
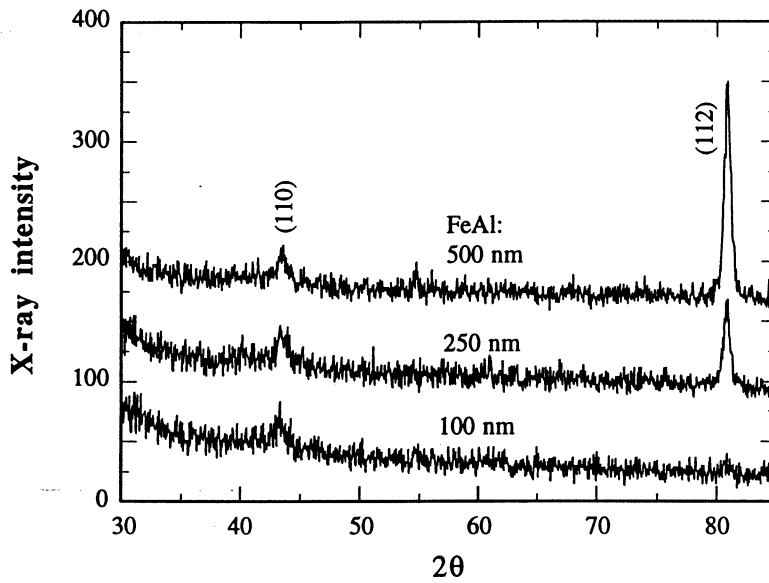
Fig. 3 The evolution of the crystallographic texture of FeAl films on smooth glass substrates.
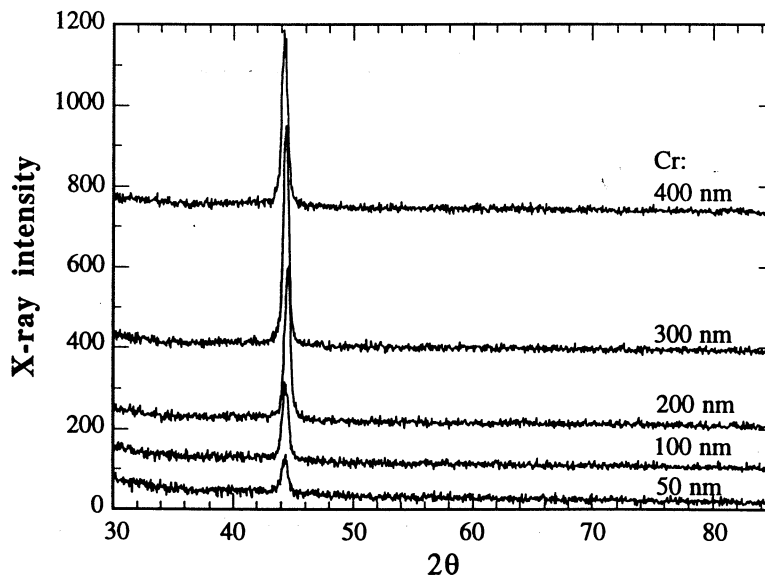
Fig. 4 The evolution of the crystallographic texture of Cr films on smooth glass substrates.
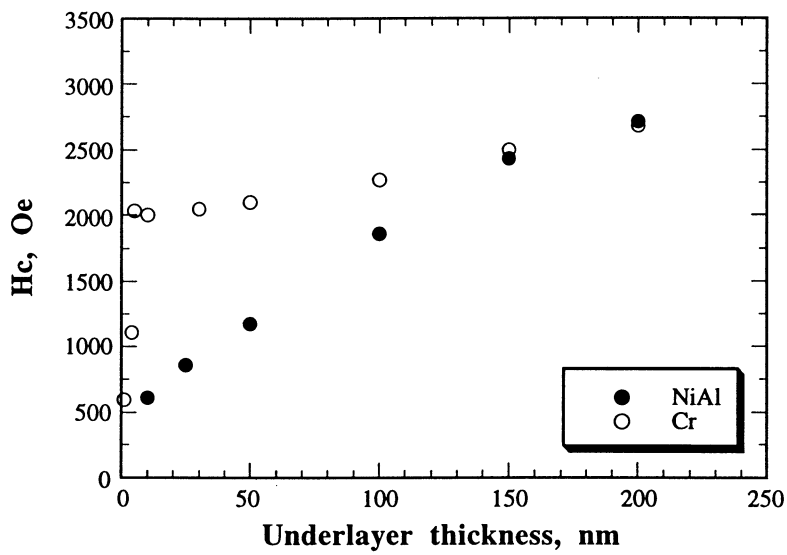
Fig. 5 Coercivity vs. underlayer thickness of 40 nm thick CoCrPt films deposited on Cr or NiAl underlayers.
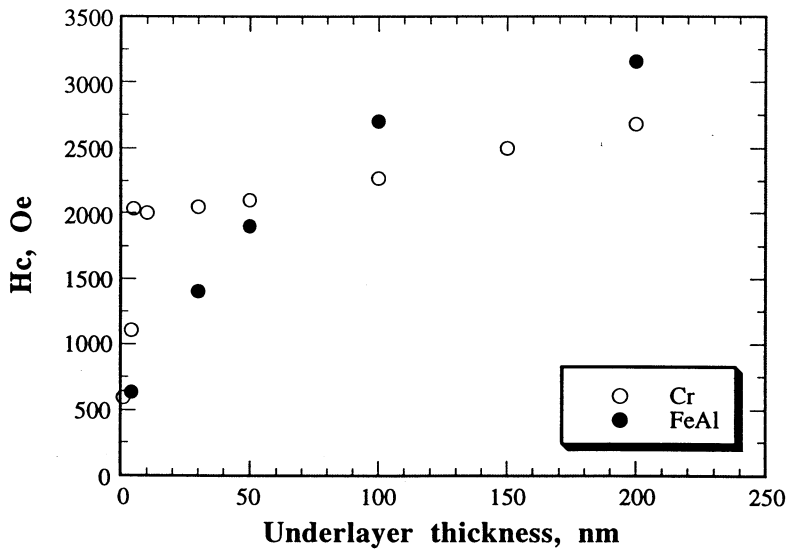
Fig. 6 Coercivity vs. underlayer thickness of 40 nm thick CoCrPt films deposited on Cr or FeAl underlayers.
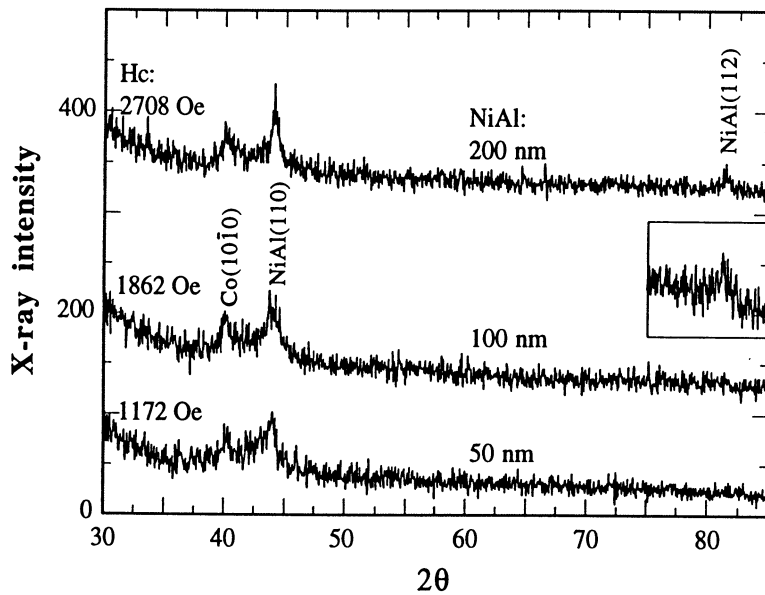
Fig. 7 X-ray diffraction spectra of 40 nm thick CoCrPt films on 50, 100 and 200 nm thick NiAl underlayers on smooth glass substrates. The insert is a portion of a slow scan of the film with a 100 nm NiAl underlayer to show the (112) peak.
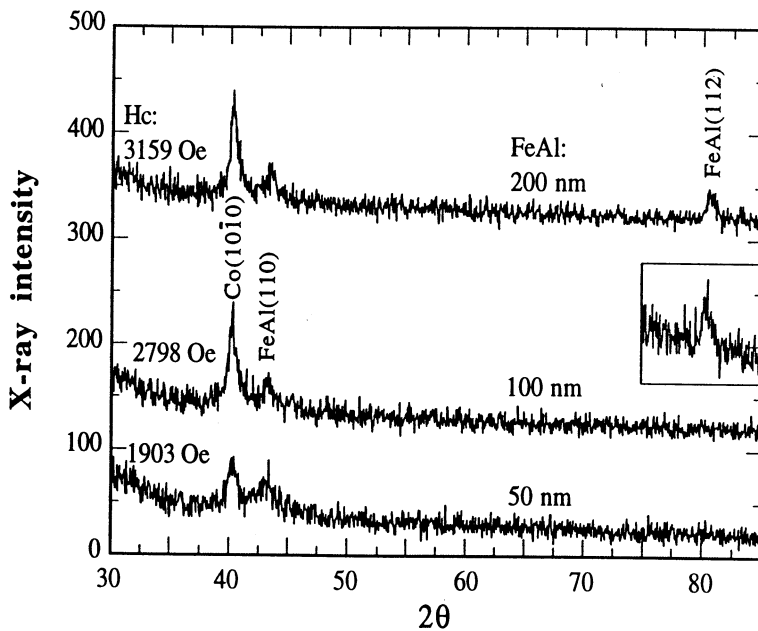
Fig. 8 X-ray diffraction spectra of 40 nm thick CoCrPt films on 50, 100 and 200 nm thick FeAl underlayers on smooth glass substrates.
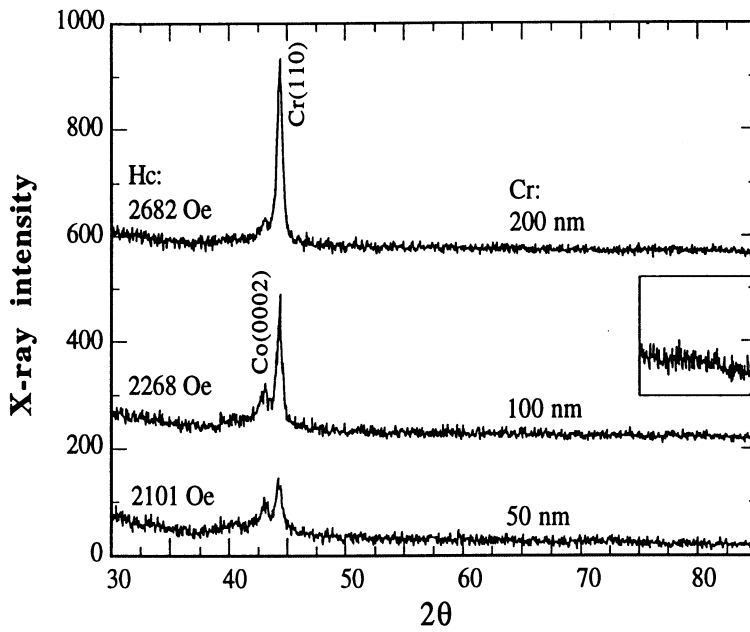
Fig. 9 X-ray diffraction spectra of 40 nm thick CoCrPt films on 50, 100 and 200 nm thick Cr underlayers on smooth glass substrates.
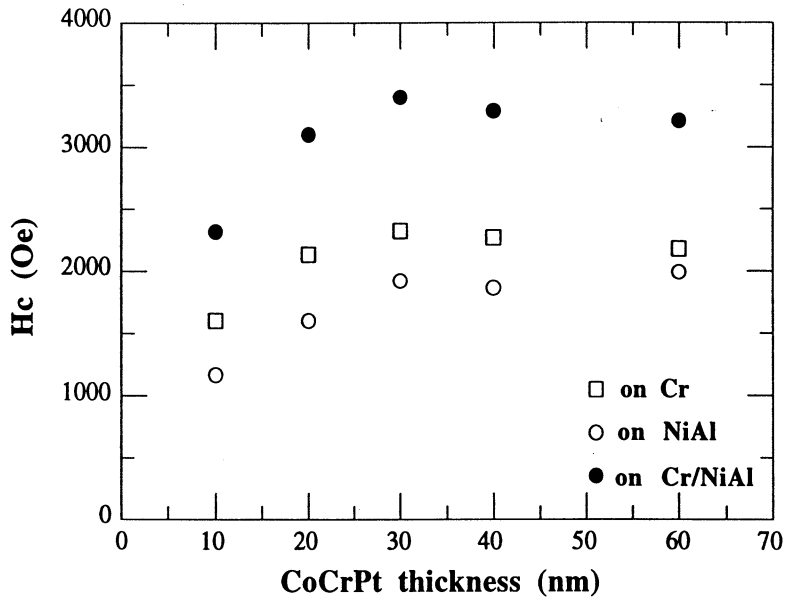
Fig. 10 In-plane coercivities of various thicknesses of CoCrPt films deposited on Cr (100 nm), NiAl (100 nm) or Cr (2.5 nm)/NiAl (100 nm) underlayers.
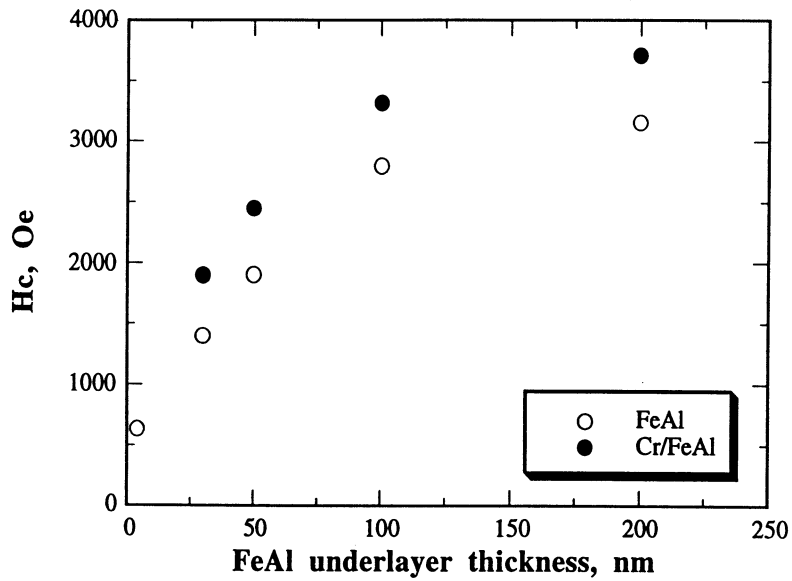
Fig. 11 In-plane coercivity vs. underlayer thickness of a 40 nm thick CoCrPt film deposited on FeAl with and without a 2.5 nm Cr intermediate layer.
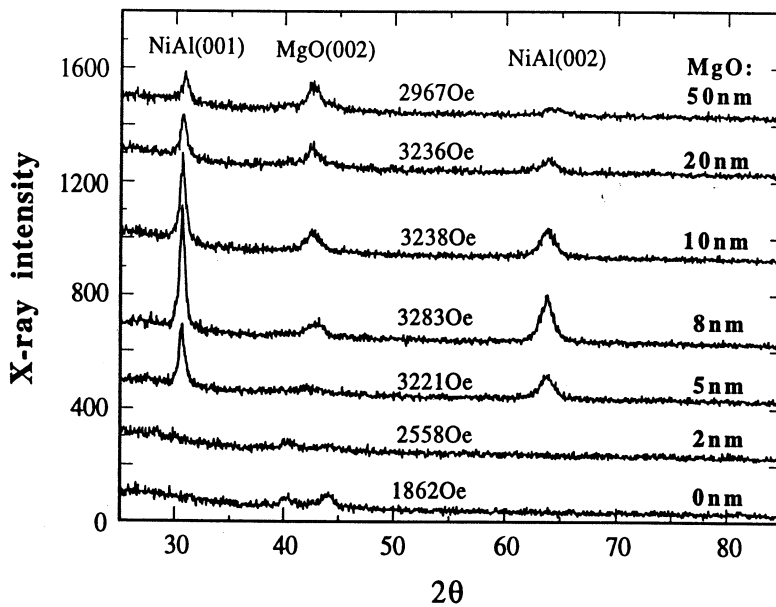
Fig. 12 X-ray diffraction spectra of the CoCrPt(40 nm)/NiAl(100 nm) films with various thicknesses of MgO seed layers.
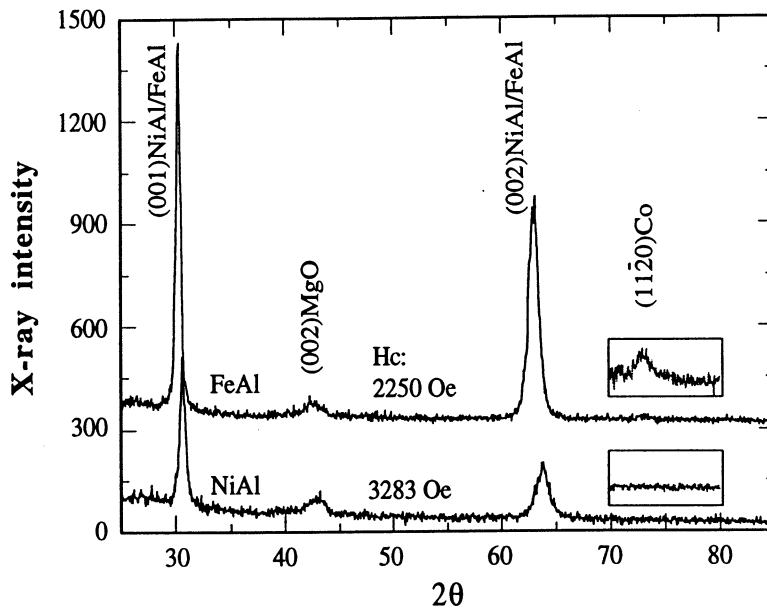
Fig. 13 X-ray diffraction spectra of CoCrPt(40 nm)/FeAl(100 nm) and CoCrPt(40 nm)/NiAl(100 nm) films on glass substrates with 8 nm thick MgO seed layers.
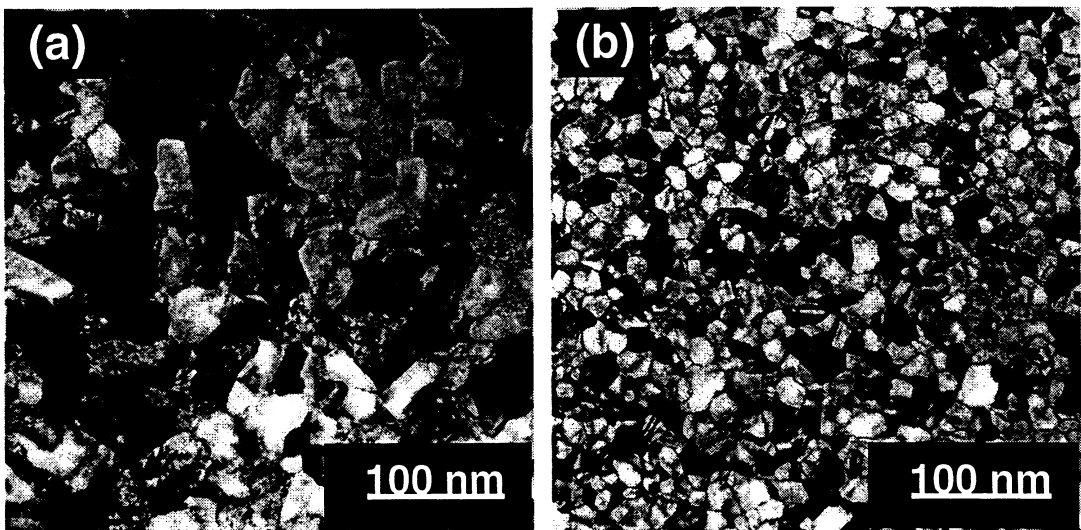

Fig. 14 Plan-view TEM bright field micrograph of a 100 nm thick NiAl film on (a) 5 nm Cr seed layer and (b) 5 nm MgO seed layer.

16
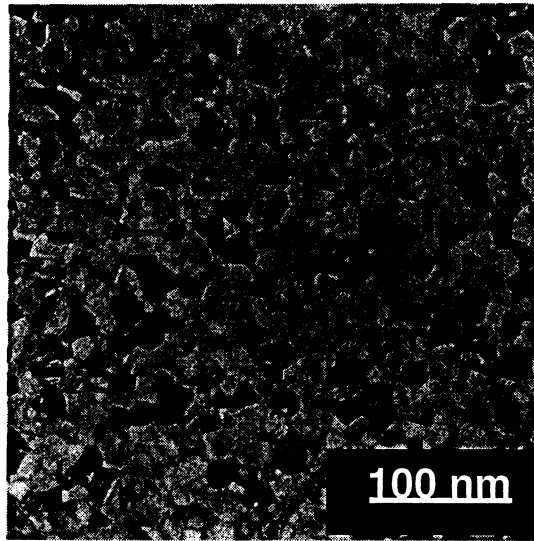
Fig. 15 Plan-view TEM bright field micrograph of a 100 nm thick NiAl film deposited on a 260°C preheated glass substrate.
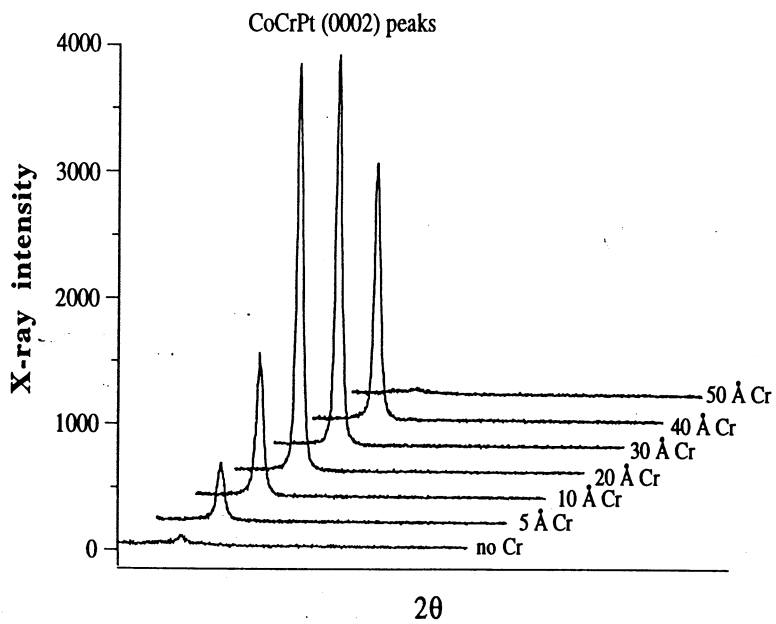

Fig. 16 X-ray diffraction spectra of 40 nm thick CoCrPt films on various thicknesses of Cr underlayers.
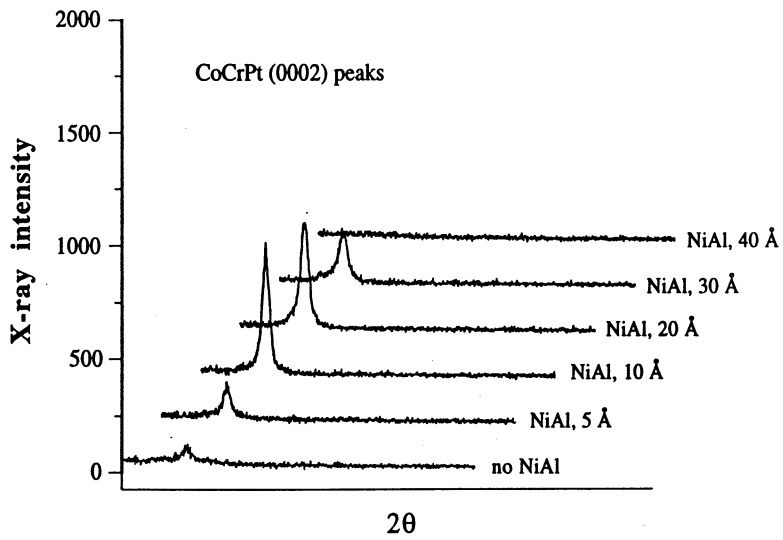
Fig. 17 X-ray diffraction spectra of 40 nm thick CoCrPt films on various thicknesses of NiAl underlayers.
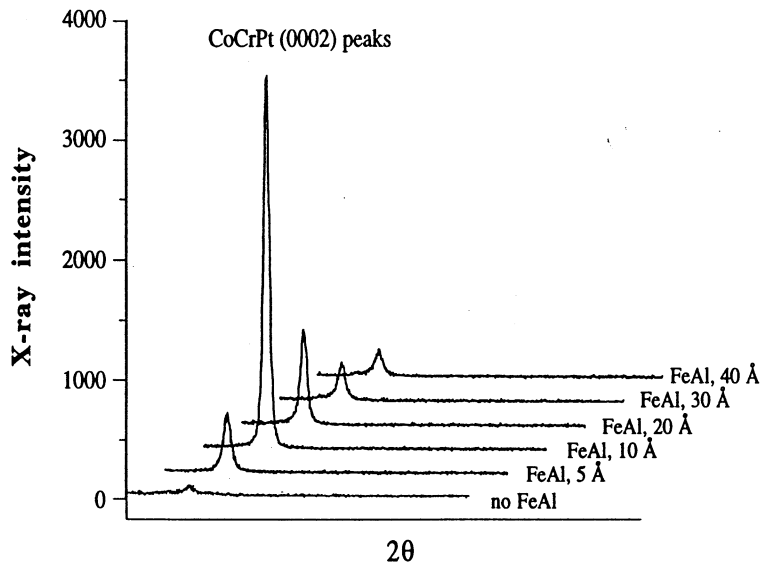

Fig. 18 X-ray diffraction spectra of 40 nm thick CoCrPt films on various thicknesses of FeAl underlayers.